Vol. 7, No. 3, November 2025 (Special Issue), pp. 359~370, p-ISSN 2685-2381, e-ISSN 2715-2626
http://dx.doi.org/10.28989/avitec.v7i3.3245

Modeling and Optimization of 4G Pathloss using Swarm Intelligence Algorithm: Case Study and Python-Based Implementation

Tri Noviyansyah, Syahfrizal Tahcfulloh*
Department of Electrical Engineering, Universitas Borneo Tarakan, Indonesia

Article Info

Article history:
Submitted August 2, 2025
Accepted August 17, 2025
Published September 23, 2025

Keywords:
Pathloss modeling;
Particle Swarm Optimization (PSO);
4G LTE networks;
radio propagation;
open-source implementation.

ABSTRACT

Accurate pathloss (PL) modeling is critical for 4G-LTE network planning in complex urban environments like Central Tarakan, Indonesia. This study presents a Python-based, open-source implementation of Particle Swarm Optimization (PSO) to calibrate three conventional PL models, Okumura-Hata, SUI, and Ericsson 9999, using real drive-test data. Initial RMSE values exceeded 50 dB, revealing severe inaccuracies under heterogeneous terrain. PSO optimization dramatically improved accuracy: RMSE reduced to 5.98 dB (Okumura-Hata, 89.44% improvement), 9.83 dB (SUI, 84.03%), and 6.44 dB (Ericsson 9999, 91.32%). The optimized Okumura-Hata model achieved the highest reliability, with 88.89% of measurement points meeting the <8 dB threshold and the lowest standard deviation (1.71 dB). Ericsson 9999 attained the lowest minimum RMSE (0.06 dB), showcasing exceptional potential under favorable conditions. PSO converged rapidly within 50 iterations, and sensitivity analysis confirmed that standard parameters (ω = 0.5–0.7, $c_1 = c_2$ = 1.8–2.2) suffice for robust calibration, eliminating need for fine-tuning. Results demonstrate that real-world propagation deviates significantly from classical logarithmic assumptions, validating the necessity of data-driven, site-specific optimization. The fully open-source framework — built with NumPy, Pandas, and Matplotlib — offers a practical, scalable solution for intelligent radio planning in dynamic urban landscapes.

Corresponding Author:
Syahfrizal Tahcfulloh,
Department of Electrical Engineering, Universitas Borneo Tarakan, Jl. Amal Lama No. 1, Tarakan 77123, Indonesia
Email: *syahfrizal@borneo.ac.id

1. INTRODUCTION

Wireless communication systems are rapidly evolving to meet the growing demand for fast, reliable, and ubiquitous data access. Simultaneously, they play a pivotal role in advancing the United Nations' 2030 Sustainable Development Goals (SDGs), particularly SDG 9 (Industry, Innovation, and Infrastructure) and SDG 11 (Sustainable Cities and Communities) [1]. A critical challenge in the design and optimization of these systems lies in modeling electromagnetic (EM) wave propagation, where signal strength typically degrades with increasing distance between transmitter and receiver due to complex environmental phenomena such as scattering, diffraction, and absorption [2][3][4][5][6].

A key parameter in wireless network planning is pathloss (PL), defined as the reduction in signal power during propagation from transmitter to receiver [7][8][9][10][11]. Research by [12] demonstrates that PL is influenced by multiple factors, including operating frequency, atmospheric conditions, terrain characteristics, and transmission distance. Traditional empirical propagation models, such as Okumura-Hata, SUI, and Ericsson 9999, are widely used for PL estimation. However, as noted by [7] and [13], their accuracy significantly diminishes in geographically complex or localized environments due to their deterministic nature and limited adaptability to site-specific conditions.

Recent advances in machine learning have introduced more flexible and data-driven alternatives for path loss prediction. Among these, Particle Swarm Optimization (PSO) has emerged as a particularly promising approach, owing to its simplicity, low computational overhead, and inherent capability for parallel search [14], [15]. While [13] have successfully applied PSO to optimize path loss models in urban settings, there remains a significant gap in literature regarding the adaptation of established empirical models, specifically Okumura-Hata, SUI, and Ericsson 9999, for 4G-LTE networks in regions characterized by unique geographical features, such as Central Tarakan.

This study addresses this gap by developing a novel, PSO-optimized path loss prediction model tailored to the environmental conditions of Central Tarakan. Our primary contributions include: (1) the design and implementation of an adaptive path loss model calibrated using PSO, and (2) a comprehensive performance evaluation comparing the proposed model against conventional propagation models under real-world measurement data. The results aim to provide a more accurate, locally optimized framework for network planning in heterogeneous geographic contexts.

2. RESEARCH METHODS

This study adopts a quantitative approach to optimize path loss (PL) models for 4G-LTE networks using the Particle Swarm Optimization (PSO) algorithm. The research methodology is structured into four distinct phases: (1) acquisition of field measurement data through drive tests, (2) simulation of conventional empirical PL models (e.g., Okumura-Hata, SUI, and Ericsson 9999), (3) optimization of model parameters via the PSO algorithm, and (4) comparative performance evaluation of the optimized models against both measured data and conventional predictions.

2.1 Field Measurement and Data Acquisition Location

Signal quality measurements were conducted along Jl. Yos Sudarso in Tarakan City, a densely built urban area with moderate traffic. Data was collected via drive test using smartphones with G-Mon Pro 1.8.6 under clear weather and at 30 km/h to minimize interference and Doppler effects, following [16]. The measurement parameters are summarized in Table 1.

Table 1. Parameters used in RF measurement

Parameters	Value
Transmit power (dBm)	38
Transmitting antenna gain (dBi)	18
Receive antenna gain (dBi)	2
Transmit antenna height (m)	30
Mobile station antenna height (m)	1.5
Band of operation	LTE Band 1, 3, 40

A drive test is a standardized field measurement technique used to evaluate the real-world performance of mobile networks by quantifying key Quality of Service (QoS) metrics. In this study, drive test data were collected, including Reference Signal Received Power (RSRP), Reference Signal Received Quality (RSRQ), and geographic coordinates, supplemented by cell identity and position data obtained from CellMapper. While RSRP measures the power level of the LTE reference signals alone (in dBm), the Received Signal Strength Indicator (RSSI) reflects the total received power across the entire bandwidth—including interference and thermal noise. RSRQ, calculated as the ratio of RSRP to RSSI, provides a more comprehensive assessment of signal quality by accounting for both signal strength and interference levels, thereby offering a better indicator of user-perceived network performance [17][18][19]. The classification of LTE signal quality levels based on these metrics is summarized in Table 2 [20][21][22][23][24][25].

Table 2. Assessment of 4G-LTE signal quality

Classification	RSRP (dBm)	RSRQ (dB)	RSSI (dBm)
Excellent	> -80	> -10	> -79
Good	-80 to -90	-10 to -15	-80 to -89
Marginal	-90 to -100	-15 to -20	-90 to -100
Poor	< -100	< -20	< -100

Following the data collection phase, the next step involves the calculation of pathloss (PL), defined as the attenuation of signal power during propagation from the transmitter to the receiver in a wireless medium. Pathloss is influenced by multiple factors, including transmission distance, physical obstructions (e.g., buildings, terrain), and environmental conditions such as atmospheric absorption, foliage density, and humidity. As radio waves propagate through space, they experience progressive power degradation due to fundamental propagation mechanisms—including free-space spreading, shadowing, diffraction, reflection, refraction, scattering, and absorption [26]. These effects collectively reduce the received signal strength below the transmitted level, necessitating accurate modeling for reliable network planning. The magnitude of path loss can be quantified using Equation (1) [27][28][29].

$$PL\ (dB) = P_{TX} + G_{TX} + G_{RX} - P_{RX} \quad (1)$$

where, P_{TX} is the transmitter power in dBm, G_{TX} is the transmitter antenna gain in dB, G_{RX} is the receiver antenna gain in dB, and P_{RX} is the received power at the receiver in dBm.

The collected pathloss (PL) data was georeferenced and visualized using Google Earth Pro to determine the Euclidean distances between each measurement point and the corresponding eNodeB. Python, leveraging libraries such as Matplotlib and GeoPandas, was employed for spatial analysis and visualization, generating a two-dimensional PL distribution map that illustrates the trend of signal attenuation as a function of distance from the base station. To estimate PL values in unmeasured locations, a 3D kriging interpolation model was applied, accounting for spatial autocorrelation across the study area. Additionally, a standard deviation map was generated to quantify spatial variability in PL, thereby identifying regions of high signal fluctuation—likely attributable to multipath interference, dense obstructions, or heterogeneous terrain. The complete data collection and processing workflow is summarized in Figure 1.

2.2 Pathloss Modeling

Following data processing, the next phase involves modeling and characterizing pathloss (PL) using established empirical propagation models. This study implements and simulates three widely adopted conventional models: Okumura-Hata, Stanford University Interim (SUI), and Ericsson 9999. The simulated PL values are then compared against the field-measured data to evaluate their accuracy under the specific environmental conditions of the study area. This comparative analysis enables the identification of systematic biases and discrepancies, offering critical insights into how local terrain features—including building density and height, vegetation coverage, and topographic variability—influence signal propagation. The ultimate objective of this step is not merely to assess model performance, but to inform the subsequent optimization process by highlighting the environmental factors that most significantly deviate from idealized assumptions in classical models.

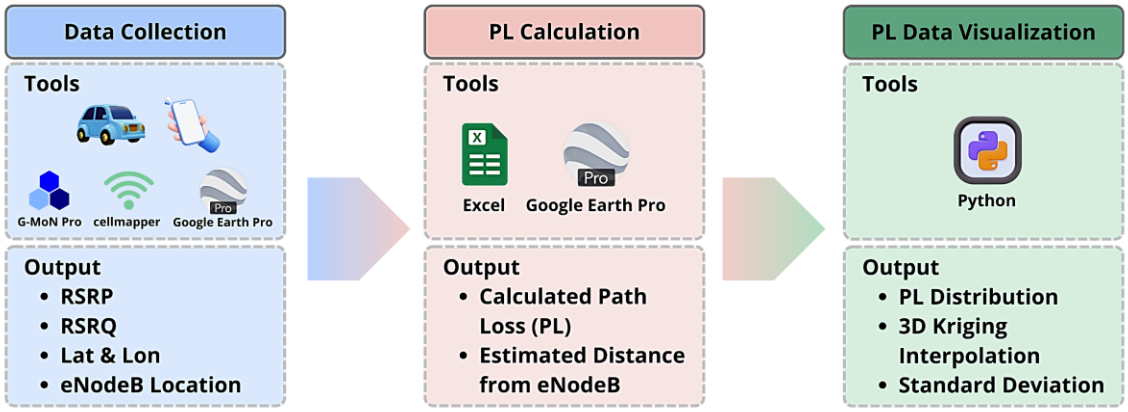

Figure 1. Workflow diagram of data collection

2.2.1 Okumura-Hata PL Model

The Okumura-Hata model is a PL prediction method originally developed based on signal strength measurements conducted in Tokyo, Japan [30]. This model is designed for estimating propagation loss in systems operating within the frequency range of 150 to 1500 MHz, with base station heights varying between 30 and 200 meters, and transmission distances ranging from 1 to 20 kilometers [20], [30]. The mathematical formulations for this PL model, tailored for urban and rural environments, are presented in Equations (2)-(11).

For urban area

$$PL_{Urban} = A + B\ log_{10}(d) - E \quad (2)$$

For suburban area

$$PL_{Suburban} = A + B\ log_{10}(d) - C \quad (3)$$

For open area

$$PL_{Open\ Area} = A + B\ log_{10}(d) - D \quad (4)$$

with

$$A = 69{,}55 + 26{,}16\ log_{10}(f_c) - 13{,}82\ log_{10}(h_b) \quad (5)$$

$$B = 44{,}9 - 6{,}55\ log_{10}(h_b) \quad (6)$$

$$C = 2(\ log_{10}(f_c/28))^2 + 5{,}4 \quad (7)$$

$$D = 4{,}78\ (log_{10}(f_c))^2 + 18{,}33\ log_{10}(f_c) - 40{,}94 \quad (8)$$

where, f_c represents the carrier frequency in MHz, d denotes the distance between the transmitter and receiver in meters, h_b indicates the eNodeB antenna height in meters, and h_r refers to the receiver antenna height in meters.

In urban areas, the value of E is determined using different formulas depending on the city type and the operating carrier frequency.

For big cities and $f_c \geq 300$ MHz,

$$E = 3{,}2\ (log_{10}(11{,}7554(h_r)))^2 - 4{,}97 \quad (9)$$

For big cities and $f_c < 300$ MHz

$$E = 8{,}29\ (log_{10}(1{,}54(h_r)))^2 - 1{,}1 \quad (10)$$

For medium to small cities

$$E = (1{,}1\ (log_{10}(f_c) - 0{,}7)h_r - (1{,}56(log_{10}(f_c) - 0{,}8) \quad (11)$$

2.2.2 Stanford University Interim (SUI) PL Model

The Stanford University Interim (SUI) pathloss propagation model is an enhanced version of the Hata model, incorporating correction parameters specifically designed for frequencies exceeding 1900 MHz. The SUI model was introduced as a practical solution for planning WiMAX networks operating in the 3.5 GHz frequency band [31]. According to research conducted by [32], the terrain types in the SUI model are categorized into three classes: Terrain A, Terrain B, and Terrain C.

Equation (12) [32] presents the mathematical formulation of the SUI pathloss model. The variables involved include: Φ as the free-space pathloss (dB), γ as the path loss exponent, d_o as the baseline distance (100 m), X_f as the frequency correction component (MHz), X_h as the tower height adjustment factor (m), and S as the shadowing component. The value of Φ at a distance of 1 meter is defined in Equation (13). Additionally, the parameter γ is calculated using Equation (14), where the constants a, b, and c are listed in Table 3. The shadowing factor S is determined based on Equation (15).

Table 3. Variations in terrain parameters for the SUI model

Category	*A*	*b*	*C*	*Φ*
A	4.6	0.0075	12.6	5.2
B	4.0	0.0065	17.1	5.2
C	3.6	0,005	20	6.6

$$PL = \Phi + 10\,\gamma\, log_{10}\left(\frac{d}{d_0}\right) + X_f + X_h + S \qquad \text{for } d > d_0 \quad (12)$$

$$A = 20\, log_{10}\left(\frac{4\pi d_0}{\lambda}\right) \quad (13)$$

$$\gamma = a - bh_b + \left(\frac{c}{h_b}\right) \quad (14)$$

$$S = 0{,}65\ (log_{10}(f_c))^2 - 1{,}3\, log_{10}(f_c) + a \quad (15)$$

Terrain-dependent adjustments for frequency and base station antenna height are expressed through correction factors presented in Equations (16) and (17).

$$X_f = 6\, log_{10}\left(\frac{f_c}{2000}\right) \quad (16)$$

$$X_h = -10{,}8\, log_{10}\left(\frac{h_r}{2000}\right) \qquad \text{for categories A and B} \quad (17)$$

$$X_h = -20\, log_{10}\left(\frac{h_r}{2000}\right) \qquad \text{for category C} \quad (18)$$

2.2.3 Ericsson 9999 PL Model

The Ericsson 9999 PL model was introduced as an enhanced version of the Okumura-Hata approach, incorporating adjustments for diverse propagation conditions. It is formulated in Equation (19), with the environment-specific coefficients α_n provided in Table 4 [33].

$$PL = \alpha_0 + \alpha_1\, log_{10}(d) + \alpha_2\, log_{10}(h_b) + \alpha_3\, log_{10}(h_b)\, log_{10}(d) - 3{,}2\ [log_{10}(11{,}75h_r)^2] + 44{,}9\, log_{10}(f_c) - 4{,}78(log_{10}(f_c))^2 \quad (19)$$

The evaluation stage followed the simulation of conventional PL models, using the Root Mean Square Error (RMSE) as the performance indicator. RMSE reflects the average discrepancy between actual measured path loss (PL_m) and model-predicted values (PL_r). A smaller RMSE signifies better model precision. In wireless propagation studies, a model is generally deemed reliable when its RMSE does not exceed 8 dB [34].

Table 4. Diverse terrain conditions applied in the Ericsson model

Condition	α_0	α_1	α_2	α_3
Rural	45.95	100.6	-12	0.1
Suburban	43.20	68.63	12	0.1
Urban	36.20	30.20	12	0.1

2.2.4 Particle-Swarm-Optimization (PSO)

Many existing path loss (PL) models suffer from limited accuracy due to their generalized, environment-agnostic formulations, which fail to account for site-specific propagation conditions. As a result, these models often exhibit significant performance degradation when applied in real-world urban, suburban, or heterogeneous terrain environments. To overcome this limitation, this study employs the Particle Swarm Optimization (PSO) algorithm to adaptively calibrate conventional PL models using field-measured data, thereby tailoring their parameters to local environmental and frequency characteristics. Originally proposed by Kennedy and Eberhart in 1995, PSO is a population-based stochastic optimization technique inspired by the coordinated motion of social organisms such as bird flocks or fish schools. In PSO, each particle represents a potential solution and iteratively updates its position and velocity based on two key influences: its own best-known position (personal best) and the best position discovered by the entire swarm (global best) [14], [39]. This adaptive search mechanism enables efficient convergence toward optimal model parameters that better reflect actual propagation behavior under complex real-world conditions.

In the PSO algorithm, each particle is identified by an index $i = 1, 2, ..., N_p$ and has a dimensionality of $j = 1, 2, ..., N_d$. During each iteration, particles update their velocity and position within the search space based on predefined mathematical rules. The updated velocity of a particle is governed by Equation (20), while its new position is determined using Equation (21). The modified velocity of the i-th particle at the $(t + 1)$-th iteration is denoted as $v_{i,j}^{(t+1)}$, and its corresponding position is represented as $X_{i,j}^{(t+1)}$. The initial values for velocity and position are expressed as $v_{i,j}^{(t)}$ and $X_{i,j}^{(t)}$, respectively. Each particle maintains a record of its best-achieved position so far, referred to as the personal best $P_{best\ i,j}^{(t)}$, and also responds to the global best position found by the entire swarm, denoted as $G_{best\ j}^{(t)}$. The updates to both velocity and position are influenced by two acceleration constants: c_1 and c_2. In this implementation, c_1 is set to 1, and c_2 is calculated as $4 - c_1$, representing the cognitive and social behavior of the particles, respectively. Additionally, two random numbers, r_{d1} and r_{d2}, uniformly distributed between 0 and 1, are introduced to incorporate stochasticity into the search process. This allows the particles to explore the solution space in a dynamic and adaptive manner [35][36].

.

$$\bar{v}_{i,j}^{(t+1)} = \bar{v}_{i,j}^{(t)} + c_1\, r_{d1}\left[\bar{P}_{best\ i,j}^{(t)} - \bar{X}_{i,j}^{(t)}\right] + c_2 r_{d2}\left[\bar{G}_{best\ j}^{(t)} - \bar{X}_{i,j}^{(t)}\right] \quad (20)$$

$$X_{i,j}^{(t+1)} = \bar{X}_{i,j}^{(t)} + \bar{v}_{i,j}^{(t+1)} \quad (21)$$

As noted by [37], the inertia weight (ω) is an essential parameter in the PSO algorithm, as it controls the trade-off between global exploration and local exploitation by adjusting the impact of P_{gbest} and P_{xbest}. Equation (22) is used to compute the inertia weight, with variables defined as follows ωt is inertia weight at the current iteration t, T denotes maximum number of iterations, and t as current iteration step.

$$\omega_t = \omega_{max} \frac{\omega_{max} - \omega_{min}}{T} t \quad (22)$$

3. RESULTS AND DISCUSSION

3.1 Geospatial Mapping of 4G-LTE Coverage Performance in Central Tarakan

Field measurements of 4G-LTE network performance were conducted along a ±2 km corridor of Jl. Yos Sudarso in Central Tarakan. The results reveal that 62.94% of measurement points exhibited excellent Reference Signal Received Power (RSRP) (> –80 dBm), 31.98% were classified as good (–90 to –80 dBm), and only 5.08% were marginal (≤ –90 dBm). In contrast, RSRQ (Reference Signal Received Quality) showed significantly lower performance: only 5.58% of locations achieved excellent quality (> –10 dB), 51.78% were rated as good (–15 to –10 dB), while a substantial 42.64% fell into the marginal range (≤ –15 dB). This discrepancy—strong RSRP coupled with low RSRQ—indicates that while signal strength is generally adequate, interference or network congestion is significantly degrading signal quality and, consequently, user-perceived reliability. The spatial distributions of RSRP and RSRQ across the study area are visualized in Figure 2 and summarized quantitatively in Table 5.

Table 5. Spatial distribution of 4G-LTE network performance on Jl. Yos Sudarso, Tarakan

Quality	RSRP (dBm)	Percentage (%)	RSRQ (dB)	Percentage (%)
Excellent	> -80	62,94	> -10	5.58
Good	-80 to -90	31,98	-10 to -15	51.78
Marginal	-90 to -100	5,08	-15 to -20	42.64
Poor	< -100	0	< -20	0

Figure 2. Mapping of RSRP levels across the research site for 4G-LTE network

Pathloss (PL) values, computed from RSRP measurements using Equation (1), ranged from 126 dB to 157 dB, with a mean value of 136.30 dB and a standard deviation of 7.65 dB, indicating a relatively homogeneous spatial distribution across the study area. Figure 3(a) presents the 3D Kriging interpolation surface of PL, where orange-to-red regions correspond to moderate pathloss (~131 dB), while blue zones represent high attenuation (>150 dB). Figure 3(b) reveals a general positive correlation between PL and distance from the eNodeB, consistent with free-space propagation trends. However, several measurement points located close to the base station exhibit unexpectedly high PL values—attributable to non-line-of-sight (NLOS) conditions, signal blockage by buildings and dense vegetation, and multipath effects. These anomalies align with findings reported in [23] and [37]–[38], which emphasize substantial signal degradation under NLOS environments due to scattering, diffraction, and absorption. The observed spatial PL patterns provide critical empirical context for evaluating the performance of conventional propagation models prior to their calibration via PSO-based optimization, as detailed in the following section.

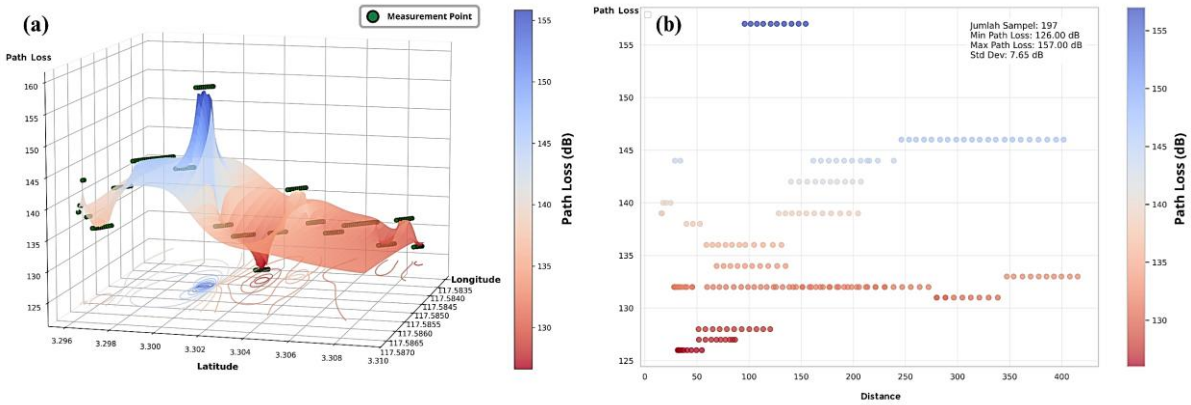

Figure 3. (a) Spatial distribution of PL using 3D Kriging on Jl. Yos Sudarso and (b) PL variation with respect to distance

3.2 Categorization of Terrain Types Using Pathloss Model Simulations

To characterize the local terrain environment, a terrain classification was performed based on the prediction performance of three conventional path loss propagation models: Okumura-Hata, Stanford University Interim (SUI), and Ericsson 9999. Each model was calibrated and evaluated against field-measured pathloss data to assess its accuracy and suitability for the heterogeneous urban and semi-urban conditions of Central Tarakan. The root mean square error (RMSE) between simulated and measured PL values was computed for each cell ID

across the study region, providing a granular evaluation of model behavior under varying local conditions. The resulting RMSE values are summarized in Table 6.

Table 6. Performance of traditional PL models in simulation

Cell-ID	RMSE (dB)								
	Okumura-Hata			SUI			Ericsson 9999		
	Urban	Suburban	Open Area	Terrain A	Terrain B	Terrain C	Urban	Suburban	Rural
324005-25	65.57	53.03	93.88	63.47	51.46	73.28	64.73	144.97	208.70
324176-11	71.01	58.99	81.28	69.06	56.50	78.86	71.25	155.50	221.42
579008-21	68.35	56.35	84.10	63.84	52.16	74.97	69.60	145.77	205.12
579008-23	75.28	62.79	80.05	76.25	62.77	84.60	73.67	166.33	239.12
579043-21	80.05	68.26	74.83	80.90	67.75	89.00	79.32	170.17	241.54
579043-23	84.67	72.19	70.75	86.52	72.75	94.39	82.73	178.01	252.96
579043-31	72.94	60.92	79.30	69.15	57.18	79.94	73.89	152.57	213.94
579176-33	84.17	71.68	71.16	85.82	72.11	93.81	82.30	177.04	251.53
699052-15	72.96	60.31	85.92	76.12	62.15	83.28	70.02	168.16	245.52

The Okumura-Hata model demonstrated the best overall performance in suburban environments, achieving an average RMSE of 63.03 dB, with 77.78% of Cell-IDs classified as optimally predicted under this setting; however, two sites exhibited better fit under open-area conditions, suggesting regional heterogeneity in propagation characteristics. The SUI model achieved the lowest overall RMSE (61.65 dB) when applied to Terrain B, indicating its relative suitability for moderately obstructed, non-urban landscapes. In contrast, the Ericsson 9999 model performed most accurately in dense urban areas (RMSE: 74.41 dB), significantly outperforming its results in rural and suburban zones (all >100 dB RMSE). Despite these relative strengths, all three conventional models exhibited consistently high RMSE values across the study region, underscoring their limited adaptability to the complex, mixed-terrain environment of Central Tarakan—characterized by variable building densities, topographic undulations, and vegetation cover. These findings corroborate the conclusions of [34], which emphasize that traditional empirical models, while useful in standardized environments, are insufficiently robust for highly heterogeneous urban settings. Consequently, there is a clear need for adaptive optimization techniques—such as PSO—to recalibrate model parameters based on local measurement data and thereby improve prediction accuracy under diverse and dynamic propagation conditions.

3.3 PSO-Based Optimization of Pathloss Propagation Models

The PSO algorithm was applied to optimize the parameters of the three propagation models—Okumura-Hata, SUI, and Ericsson 9999. A comprehensive tuning process was performed by varying key PSO parameters, such as iteration count, swarm population, inertia weight (ω), cognitive coefficient (c_1), and social coefficient (c_2), to achieve the best possible model performance. Table 7 presents the selected parameter configurations used for optimizing each PL model.

The exploration results summarized in Table 7 reveal consistent behavioral trends across all three pathloss models following PSO optimization: (1) Rapid convergence was observed within the first 50 iterations, with the majority of RMSE reduction occurring during the initial 10–20 iterations—indicating efficient exploitation of the search space early in the optimization process; (2) While swarm size had negligible impact on the final RMSE (i.e., solution quality), it exerted a pronounced effect on computational efficiency: increasing the swarm population from 20 to 150 resulted in a 5-10-fold increase in runtime, without commensurate improvement in accuracy; (3) Sensitivity analyses of the key PSO parameters (inertia weight ω, cognitive coefficient c_1, and social coefficient c_2) revealed only marginal variations in RMSE performance across tested ranges, suggesting that the objective function's search landscape is characterized by a broad, well-defined global optimum basin. These findings imply that near-optimal PL model calibration can be reliably achieved using relatively simple, robust parameter settings — specifically, $\omega = 0.5–0.7$, $c_1 = 1.8–2.2$, and $c_2 = 1.8–2.0$ — thereby obviating the need for extensive, computationally expensive hyperparameter tuning. This practical insight enhances the feasibility of deploying PSO in real-world network planning scenarios. A comparative summary of the optimized model performances is presented in Table 8, while the original and post-optimization parameter values for each conventional propagation model are detailed in Table 9.

The optimization of conventional pathloss (PL) models using the Particle Swarm Optimization (PSO) algorithm yielded substantial improvements in prediction accuracy across all three models, as summarized in Table 8. For the Okumura-Hata model, the average RMSE was reduced from 56.64 dB to 5.98 dB — a dramatic improvement of 89.44%. Following optimization, this model exhibited the most consistent performance, with the lowest standard deviation (1.71 dB) and 88.89% of Cell-IDs achieving RMSE values below the 8 dB threshold, indicating high reliability under diverse local conditions. The SUI model also demonstrated significant enhancement, with average RMSE decreasing from 61.56 dB to 9.83 dB (84.03% improvement). However, its

performance was less uniform: only 44.44% of measurement points met the 8 dB accuracy criterion, and the higher standard deviation (4.21 dB) suggests greater sensitivity to spatial variability in terrain and obstruction patterns, reflecting comparatively lower adaptability to Central Tarakan's heterogeneous environment. Most strikingly, the Ericsson 9999 model underwent the most transformative improvement, achieving the highest percentage error reduction (91.32%), with average RMSE plummeting from 74.17 dB to just 6.44 dB—outperforming both Okumura-Hata and SUI in absolute accuracy. Notably, after PSO optimization, Ericsson 9999 attained the lowest minimum RMSE value (0.06 dB) among all models, revealing its strong potential for achieving near-perfect predictions under favorable propagation conditions. Despite its poor initial performance, this model's capacity for fine-grained adaptation highlights its untapped predictive capability when calibrated with field data.

Table 7. PSO tuning settings and execution efficiency in PL model optimization

Parameter	Okumura-Hata	SUI	Ericsson 9999
Optimal iteration count	50	50	50
RMSE at the first iteration	7.74 dB	9.37 dB	3.60 dB
Converged RMSE value	5.73 dB	9.37 dB	2.78 dB
Optimal swarm size	20	20	20
Computation time (with swarm size 20)	0.52 s	0.60 s	0.56 s
Computation time (with swarm size 150)	6.03 s	3.93 s	4.06 s
Optimized PSO configuration			
• Inertia weight (ω)	0.7	0.5	0.5
• Cognitive coefficient (c_1)	1.8	2.2	2.0
• Social coefficient (c_2)	1.8	2.0	2.0

Table 8. Performance assessment of PL models based on statistical errors

Statistic	Okumura-Hata		SUI		Ericsson 9999	
	Without PSO	With PSO	Without PSO	With PSO	Without PSO	With PSO
Mean (dB)	56.64	5.98	61.56	9.83	74.17	6.44
Median (dB)	60.92	5.57	62.15	9.38	73.67	7.03
Min (dB)	7.47	4.08	51.46	4.46	64.73	0.06
Max (dB)	71.16	9.46	72.75	15.64	82.73	10.81
Std. Dev	18.37	1.71	7.42	4.21	5.79	3.33
Skewness	-1.99	0.74	0.13	0.27	0.15	-0.54
Kurtosis	2.80	-0.60	-1.34	-1.46	-1.11	-0.80
% < 8dB	88.89		44.44		44.44	
% Improvement	89.44		84.03		91.32	

Table 9. PL model parameters before and after PSO optimization

Model	A1	A2	A3	B1	B2	E1	E2	E3	E4
O-H	69.55	26.16	13.82	12.6	44.9	6.55	0.7	1.56	0.8
O-H PSO	40	28.39	20	30	10	1.04	0.9	3	2

Model	A	B	C
SUI A	4.6	0.0075	12.6
SUI B	0.0075	0.0065	17.1
SUI C	12.6	0.005	20
SUI PSO	3.966	0.070	23.191

Model	a_0	a_1	a_2	a_3
Eric Ur	36.20	30.20	12	0.1
Eric SU	43.20	68.63	12	0.1
Eric Ru	45.95	100.6	12	0.1
Eric PSO	28.755	0.875	11.209	0.030

Statistical analysis reveals a pronounced shift in the error distribution of the Okumura-Hata model following PSO optimization. Skewness evolved from –1.99 to 0.74, indicating a transition from a left-skewed (high-RMSE tail) to a near-symmetric or slightly right-skewed distribution—reflecting a significant reduction in the frequency of large prediction errors. Kurtosis shifted from a positive value of 2.80 (leptokurtic, heavy-tailed) to –0.60 (platykurtic), signaling a more uniform and dispersed error profile, with fewer extreme outliers. Prior to optimization, the model exhibited optimal performance in suburban environments, consistent with its original empirical derivation. However, after PSO calibration, urban areas emerged as the region with the highest accuracy, suggesting that the algorithm successfully reweighted model parameters to better capture the complex propagation characteristics of Central Tarakan's built-up environment—including dense infrastructure, variable building heights, and multipath effects. Although all three models benefited from PSO-based optimization, the recalibrated Okumura-Hata model delivered the most consistent and reliable predictions, achieving the highest proportion of Cell-IDs (88.89%) with RMSE ≤ 8 dB—a threshold widely regarded as indicative of acceptable network planning accuracy. This superior reliability underscores its suitability for practical deployment in heterogeneous urban-suburban landscapes. Critically, these results demonstrate that real-world signal behavior in Central Tarakan deviates significantly from the idealized logarithmic assumptions inherent in conventional propagation models. The marked improvement achieved through data-driven calibration strongly supports the necessity of adopting site-specific, optimization-based approaches for accurate path loss estimation in complex, non-standard environments.

This study presents a practical implementation of the Particle Swarm Optimization (PSO) framework originally introduced by Kennedy and Eberhart [14], extending its application to the calibration of empirical path loss models in complex 4G-LTE environments. While prior work by [13] highlights the inherent limitations of conventional propagation models when applied without adaptation, this paper addresses that gap through a data-driven, algorithmically enhanced optimization approach. Furthermore, insights from [37] on improved convergence strategies—such as the use of Fuzzy Enhanced Inertia Weight (FEIW)—suggest promising avenues for future refinement. Collectively, this work represents a natural synthesis and evolution of three foundational contributions: it builds upon the conceptual foundation of PSO from [14], incorporates algorithmic enhancements from [37], and leverages the empirical modeling framework established in [13]. By unifying these elements into a cohesive, field-validated methodology, this study advances the state of the art in site-specific path loss prediction—demonstrating how intelligent optimization can bridge the gap between theoretical models and real-world propagation dynamics in heterogeneous urban landscapes such as Central Tarakan.

4. CONCLUSION

This study assessed the 4G-LTE network performance in Tarakan using signal quality mapping and PL estimation. While RSRP indicated good to excellent signal strength, RSRQ revealed vulnerability to interference. PL values varied significantly due to LOS/NLOS conditions influenced by buildings and vegetation. Three conventional models — Okumura-Hata, SUI, and Ericsson 9999 — showed poor accuracy, with RMSE values far exceeding the 8 dB threshold. Applying Particle Swarm Optimization (PSO) greatly improved prediction accuracy. The optimized Okumura-Hata model performed best, achieving an average RMSE of 5.98 dB, with 88.89% of Cell-IDs meeting the 8 dB criterion. Ericsson 9999 showed the highest improvement (91.32%), while SUI remained sensitive to geographical variations. PSO-based optimization effectively recalibrated model parameters for local conditions. The PSO-enhanced Okumura-Hata model is recommended for accurate PL estimation in complex urban environments like Tarakan, highlighting the value of data-driven optimization in propagation modeling. Based on the findings of this study, the next development direction is the application of this Particle Swarm Optimization (PSO)-based optimization framework to 5G networks, particularly for modeling path loss in urban environments with complex and heterogeneous topography. The data-driven approach, proven effective in improving propagation model accuracy in 4G-LTE networks in Tarakan, can be further developed to accommodate higher frequencies and beamforming technologies in 5G networks. Furthermore, variations in environmental conditions such as building density, structure height, and the use of massive MIMO should be integrated into the model to enhance prediction realism. Aligned with the recommendations of [34], which emphasize the importance of analyzing model stability and adaptability under dynamically changing environmental conditions, future research could extend model validation across various urban, suburban, and rural scenarios using empirical datasets from broader geographical regions, aiming to establish a more universal yet locally sensitive modeling framework. While the PSO method itself is not part the study of [13], the scientific direction proposed in the statement is highly consistent with the article's contributions and recommendations. The measured D-band channel data, reflection characteristics, and angular analysis provide the empirical basis needed to build advanced, adaptive, and environment-aware propagation models for future 5G/6G FWA systems—exactly what the statement envisions.

REFERENCE

[1] K. Ojutkangas, E. Rossi, S. Aalto, and M. Matinmikko-Blue, "Linking mobile communications with the United Nations sustainable development goals: Mapping process," Discussion Paper, Centre for European Policy Studies,2020. [Online]. Available: https://www.econstor.eu/handle/10419/224869

[2] S. R. Saunders and A. A. Aragón-Zavala, *Antennas and Propagation for Wireless Communication Systems*. Hoboken, NJ, USA: John Wiley & Sons, 2024.

[3] S. Kumar, *Wireless Communication – The Fundamental and Advanced Concepts*. Aalborg, Denmark: River Publishers, 2022.

[4] M. Khalily, O. Yurduseven, T. J. Cui, Y. Hao, and G. V. Eleftheriades, "Engineered electromagnetic metasurfaces in wireless communications: Applications, research frontiers and future directions," *IEEE Commun. Mag.*, vol. 60, no. 10, pp. 88–94, 2022. https://dx.doi.org/10.1109/MCOM.004.2200052

[5] A. M. Ado, M. I. Zubair, and A. A. Wakili, "Attenuations in wireless radio communication," *Int. J. Res. Appl. Sci. Eng. Technol.*, vol. 8, pp. 2520–2524, 2020. https://dx.doi.org/10.22214/ijraset.2020.5418

[6] A. Saakian, *Radio Wave Propagation Fundamentals*. Norwood, MA, USA: Artech House, 2020.

[7] O. E. Jackson, M. Uthman, and S. Umar, "Performance analysis of path loss prediction models on very high frequency spectrum," *Eur. J. Eng. Technol. Res.*, vol. 7, no. 2, pp. 87–91, 2022. https://dx.doi.org/10.24018/ejeng.2022.7.2.2783

[8] S. Ojo, M. Akkaya, and J. C. Sopuru, "An ensemble machine learning approach for enhanced path loss predictions for 4G LTE wireless networks," *Int. J. Commun. Syst.*, vol. 35, no. 7, p. e5101, 2022. https://dx.doi.org/10.1002/dac.5101

[9] O. E. Ogunsola, O. Adekele, and O. I. Olaluwoye, "Mobile 4G LTE networks mobility and coverage for some locations in Ibadan using path loss analysis," *IEEE Comput. Soc. Tech. Paper Ser.*, vol. 26, pp. 7–22, 2020. https://dx.doi.org/10.22624/isteams/v26p2-ieee-ng-ts

[10] A. Akinbolati and M. O. Ajewole, "Investigation of path loss and modeling for digital terrestrial television over Nigeria," *Heliyon*, vol. 6, no. 6, 2020. https://dx.doi.org/10.1016/j.heliyon.2020.e04101

[11] A. A. Olukunle, A. O. Kunle, O. O. Joel, I. A. Okikiade, A. M. Olusegun, and A. S. Adeola, "Development of a modified propagation model of a wireless mobile communication system in a 4G network," *Int. J. Electr. Comput. Eng.*, vol. 13, no. 6, pp. 6489–6500, 2023. https://dx.doi.org/10.11591/ijece.v13i6.pp6489-6500

[12] A. Bouchemha, H. Djellab, and M. C. Nait-Hamoud, "Analysis and optimization of 4G/LTE network pathloss using particles swarm optimization algorithm," *Int. J. Electr. Electron. Res.*, vol. 12, no. 2, pp. 557–566, 2024. https://dx.doi.org/10.37391/IJEER.120230

[13] B. D. Beelde, E. Tanghe, D. Plets, and W. Joseph, "Outdoor channel modeling at d-band frequencies for future fixed wireless access applications," *IEEE Wireless Commun. Lett.*, vol. 11, no. 11, pp. 2355–2359, 2022. https://dx.doi.org/10.1109/LWC.2022.3202921

[14] T. M. Shami, A. A. El-Saleh, M. Alswaitti, Q. Al-Tashi, M. A. Summakieh, and S. Mirjalili, "Particle swarm optimization: A comprehensive survey," *IEEE Access*, vol. 10, pp. 10031–10061, 2022. https://dx.doi.org/10.1109/ACCESS.2022.3142859

[15] A. G. Gad, "Particle swarm optimization algorithm and its applications: A systematic review," *Arch. Comput. Methods Eng.*, vol. 29, no. 5, pp. 2531–2561, 2022. https://dx.doi.org/10.1007/s11831-021-09694-4

[16] Z. Shakir, A. Y. Mjhool, A. Al-Thaedan, A. Al-Sabbagh, and R. Alsabah, "Key performance indicators analysis for 4G-LTE cellular networks based on real measurements," *Int. J. Inf. Technol.*, vol. 15, pp. 1347–1355, 2023. https://dx.doi.org/10.1007/s41870-023-01210-0

[17] R. A. Sulaiman and Y. Saragih, "Analisis quality of service (QoS) jaringan provider indihome melalui drive test di kabupaten subang [Analysis of Indihome provider network quality of service (QoS) through drive testing in Subang Regency]," *Aisyah J. Inf. Electr. Eng.*, vol. 6, no. 1, pp. 110–117, 2024. https://dx.doi.org/10.30604/jti.v6i1.219 (in Indonesian).

[18] L. M. Silalahi, S. Budiyanto, F. A. Silaban, I. U. V. Simanjuntak, and A. D. Rochendi, "Improvement of quality and signal coverage LTE in Bali province using drive test method," in *Proc. Int. Seminar Intell. Technol. Appl.* (ISITIA), Surabaya, Indonesia, 2021, pp. 376–380. https://dx.doi.org/10.1109/ISITIA52817.2021.9502227

[19] Y. Mahendra, S. M. A. Sasongko, and M. S. Yadnya, "Analisis hasil pengukuran quality of service (QoS) dan kuat sinyal 4G LTE pada kondisi line of sight (LOS) dan kondisi non line of sight (NLOS) di daerah urban studi kasus (lingkungan Universitas Mataram) [Analysis of 4G LTE Quality of Service (QoS) and Signal Strength Measurement Results under LOS and NLOS in an Urban Area: Case Study at University of Mataram]," *J. Media Informatika*, vol. 6, no. 2, pp. 688–695, 2024. [Online] Available: https://ejournal.sisfokomtek.org/index.php/jumin/article/view/4800 (in Indonesian).

[20] M. Ayad, R. Alkanhel, K. Saoudi, M. Benziane, S. Medjedoub, and S. S. M. Ghoneim, "Evaluation of radio communication links of 4G systems," *Sensors*, vol. 22, no. 10, p. 3923, 2022. https://dx.doi.org/10.3390/s22103923
[21] M. Rani, S. Aulia, and Zurnawita, "Analysis of measuring drive test result 4G LTE network telkomsel operators using tems pocket and tems discovery software," *Int. J. Telecommun. Electron. Comput. Sci.*, vol. 1, no. 1, pp. 22–28, 2024.
[22] M. Gharib, S. Nandadapu, and F. Afghah, "An exhaustive study of using commercial LTE network for UAV communication in rural areas," in *Proc. IEEE Int. Conf. Commun. Workshops* (ICC Workshops), 2021, pp. 1–6. https://dx.doi.org/10.1109/ICCWorkshops50388.2021.9473547
[23] M. Behjati, M. A. Zulkifley, H. A. H. Alobaidy, R. Nordin, and N. F. Abdullah, "Reliable aerial mobile communications with RSRP & RSRQ prediction models for the Internet of Drones: A machine learning approach," *Sensors*, vol. 22, no. 15, p. 5522, 2022. https://dx.doi.org/10.3390/s22155522
[24] I. Joseph, E. Oghu, and O. O. Roberts, "Path loss and models: A survey and future perspective for wireless communication networks," *Int. J. Adv. Netw. Appl.*, vol. 15, no. 2, pp. 5892–5907, 2023. https://dx.doi.org/10.35444/IJANA.2023.15209
[25] F. A. I. Nuari, U. K. Usman, and A. T. Hanuranto, "Penerapan Unmanned Aerial Vehicle (UAV) untuk Pengukuran Kuat Sinyal (Drive Test) pada Jaringan 4G LTE [Application of Unmanned Aerial Vehicle (UAV) for Signal Strength Measurement (Drive Test) in 4G LTE Networks]," *AVITEC*, vol. 3, no. 1, pp. 69–82, Feb. 2021. https://dx.doi.org/10.28989/avitec.v3i1.893 (in Indonesian).
[26] A. Barrios-Ulloa, A. Cama-Pinto, E. De-la-Hoz-Franco, R. Ramírez-Velarde, and D. Cama-Pinto, "Modeling of path loss for radio wave propagation in wireless sensor networks in cassava crops using machine learning," *Agriculture*, vol. 13, no. 11, p. 2046, 2023. https://dx.doi.org/10.3390/agriculture13112046
[27] S. Tahcfulloh, E. Wahyuni, D. Santoso, and A. S. Anam, "Radiowave pathloss modeling using polynomial methods for wet and dry land and rice agriculture," in *Proc. 11th Int. Conf. Electr. Eng., Comput. Sci. Informatics* (EECSI), Yogyakarta, Indonesia, 2024, pp. 379–384. https://dx.doi.org/10.1109/EECSI63442.2024.10776287
[28] B. Myagmardulam, N. Tadachika, K. Takahashi, R. Miura, F. Ono, and T. Kagawa, "Path loss prediction model development in a mountainous forest environment," *IEEE Open J. Commun. Soc.*, vol. 2, pp. 2492–2501, 2021. https://dx.doi.org/10.1109/OJCOMS.2021.3122286
[29] J. Wang, Y. Hao, and C. Yang, "The current progress and future prospects of path loss model for terrestrial radio propagation," *Electronics*, vol. 12, no. 24, p. 4959, 2023. https://dx.doi.org/10.3390/electronics12244959
[30] T. I. Unger and M. Kuczmann, "Comparison of outdoor radiowave propagation models for land mobile systems in the 3.6 GHz and 6 GHz frequency bands," *Telecom*, vol. 6, no. 2, pp. 1–41, 2025. https://dx.doi.org/10.3390/telecom6020042
[31] A. Akinbolati and B. T. Abe, "Investigating the reliability of empirical path loss models over digital terrestrial UHF channels in Ikorodu and Akure, southwestern Nigeria," *Telecom*, vol. 6, no. 2, pp. 1–21, 2025. https://dx.doi.org/10.3390/telecom6020028
[32] P. D. Katev, "Propagation models for WiMAX at 3.5 GHz," in *Proc. ELEKTRO*, Rajecke Teplice, Slovakia, 2012, pp. 61–65. https://dx.doi.org/10.1109/ELEKTRO.2012.6225572
[33] E. M. D. Djomadji, I. B. Kabiena, J. T. Mandengue, F. Watching, and E. Tonye, "Okumura Hata propagation model optimization in 400 MHz band based on differential evolution algorithm: Application to the city of Bertoua," *J. Comput. Commun.*, vol. 11, no. 5, pp. 52–69, 2023. https://dx.doi.org/10.4236/jcc.2023.115005
[34] S. K. Meena and A. R. Garg, "Stability analysis of optimized PMU placement using hybrid and individual TLBO-PSO techniques," *Adv. Sustain. Sci. Eng. Technol.*, vol. 7, no. 1, pp. 02501024–02501024, 2025. https://dx.doi.org/10.26877/asset.v7i1.1261
[35] K. Jegadeeswari and R. Rathipriya, "Optimized stacking ensemble classifier for early cancer detection using biomarker data," *Adv. Sustain. Sci. Eng. Technol.*, vol. 6, no. 4, pp. 02404017–02404017, 2024. https://dx.doi.org/10.26877/asset.v6i4.986
[36] S. Tahcfulloh, E. Wahyuni, D. Santoso, and R. Juliannanda, "Modified COST-235 empirical pathloss model for agricultural WSN using particle swarm optimization," *IIUM Eng. J.*, vol. 26, no. 1, pp. 336–352, 2025. https://dx.doi.org/10.31436/iiumej.v26i1.3446
[37] M. J. Amoshahy, M. Shamsi, and M. H. Sedaaghi, "A novel flexible inertia weight particle swarm optimization algorithm," *PLoS ONE*, vol. 11, no. 8, p. e0161558, 2016. https://dx.doi.org/10.1371/journal.pone.0161558
[38] R. S. Kaffa, U. K. Usman, Z. S. L. Purnomo, R. F. Akbar, and S. P. Wisetyo, "Network signal coverage expansion planning WLAN outdoor with 4-C scenario approach at Telkom University," *Aviation*

Electronics, Information Technology, Telecommunications, Electricals, and Controls (*AVITEC*), vol. 7, no. 1, pp. 87–102, Feb. 2025. https://dx.doi.org/10.28989/avitec.v7i1.2711

[39] J. Kennedy and R. Eberhart, "Particle swarm optimization," in *Proc. ICNN'95 – Int. Conf. Neural Netw.*, Perth, WA, Australia, 1995, vol. 4, pp. 1942–1948. https://dx.doi.org/10.1109/ICNN.1995.488968